Proceedings of the 1st International Conference in Fluid Thermal and Energy Systems
June 9-11, 2022, NIT Calicut, Kerala, India
ICFTES2022–ES–126

Effect of internal flow channels on encapsulated PCM with constant volume

Shivam Kumar Pandey[1], Kartik Tewari[1], Vidula Athawale[1], and Anirban Bhattacharya[1,*]

[1]School of Mechanical Sciences, IIT Bhubaneswar, Odisha-752050, India

*Corresponding author email: anirban@iitbbs.ac.in

ABSTRACT

A numerical study is presented to analyze the effect of internal flow channels on latent heat thermal energy storage (LHTES) systems with encapsulated phase change materials (PCMs) while maintaining constant PCM volume. A 3D cubical domain is modeled with a PCM capsule located at its center subjected to hot heat transfer fluid (HTF). Internal channels are made into the PCM capsules to improve the melting rate. Maintaining a constant volume makes the total latent energy stored constant although the rate of energy storage varies with change of internal radius. The model also captures the natural convection within the capsules. Coupled fluid flow and enthalpy model is used to solve the flow of HTF and phase change process of PCM. Capsules with base radii of 4 mm and 8 mm are studied under four different configurations with the ratio of the channel to the base radius (r/R_0) varying as 0.250, 0.333, 0.416, and 0.500. The results show that the melting duration reduces by 42.58% for the capsule with a 4 mm base radius when r/R_0 is 0.500. Similarly, the melting duration reduces by 51.15% with an 8 mm base radius when r/R_0 is 0.500. For all r/R_0 ratios it is found that the effect of internal channels on energy storage rates and melting time are considerably more for the larger capsule size.

Keywords: Energy storage; Encapsulated PCM; Internal channels; Heat transfer enhancement.

1. INTRODUCTION

Phase Change Material (PCM), a latent energy storage technique, allows energy storage while showing a negligible change in the temperature of the material used. PCMs are stable chemically and safe for the environment. To increase the thermal conductivity of PCMs and improve the latent energy storage ability, various techniques are available in the literature. A few of which include encapsulation of PCM, including metal fins, and using carbon or silver nanoparticles. Besides solar energy storage, they are also widely implemented in textiles, buildings, and thermal management systems for batteries.

2. LITERATURE REVIEW AND OBJECTIVE

The literature shows that significant work has been conducted on encapsulated PCM-based energy storage systems. However, very few works have highlighted the effect of enhancing latent energy storage rate by making minor modifications to the PCM capsule geometry.

A computational investigation by Khodadadi and Zhang involved analyzing the melting of PCM within an encapsulation under the influence of combined conduction and buoyancy-driven convection [1]. Regin et al. [2] conducted studies to determine the role of natural convection and phase-change temperature on the heat transfer of a cylindrically encapsulated PCM with varying capsule radii. Three stages of melting were analysed both numerically and experimentally.

Kalaiselvam et al. [3] conducted an analytical study to determine the location of the transient interface for solidification and melting. The time for attaining steady-state and solidification characteristics were both explained using a non-dimensional heat generation parameter. Agyenim et al. [4] reviewed materials and container geometries proposed earlier to store PCMs. Container geometries, resembling day-to-day engineering systems, such as long thin heat pipes, cylindrical or rectangular containers, were used to simulate the melting of PCMs. The lowest heat losses were minimal from the shell and tube systems. Hlimi et al. [5] conducted a numerical investigation on encapsulated gallium placed inside a horizontal cylinder. The key observation was that in the later stages of the process, unsymmetrical melting occurred along the horizontal axis of the capsule. Liu et al. [6], presented a review of the macro-encapsulated PCMs for buildings. The paper compared the merits and limitations of micro and macro encapsulation methods. It also emphasized the importance of geometry and material selection on PCM's overall phase change characteristics.

Energy storage characteristics of PCMs installed within a water tank were analyzed numerically and experimentally by Bony and Citherlet [7]. A variety of geometries and material combinations for the PCMs were considered. A study on spherically encapsulated PCM was conducted by Sattari et al. [8] with varying operating conditions and PCM container diameters. The results indicated that the change in surface temperature has more influence on melting

duration, melting rates, and overall heat transfer compared to other process parameters such as the container's diameter and the initial PCM temperature.

Our present work analyzes the energy storage characteristics of encapsulated PCMs with internal channels through the development of a 3D finite volume-based model. For each case, the total volume of the PCM with an internal channel is maintained constant and equal to the volume of the corresponding capsule with no channel. Thus, by choosing fixed set of values for the channel radius, the value of PCM's outer diameter is determined. It was found from the literature that the central region of a spherically encapsulated PCM takes a long time to melt completely. In order to improve the rate of energy storage, the inclusion of such channels into the PCMs is proposed.

3. MATHEMATICAL MODEL

All the simulations are performed in a three-dimensional cubical domain of size 20×20×20 mm^3, which along with boundary conditions, is represented in Figure 1. Simulations are conducted on a paraffin wax-based single capsule. The heat transfer fluid i.e., water, flows from the bottom to the top across the domain, with a constant inlet temperature of 373 K. The domain is initially maintained at 303 K. As soon as the heat transfer fluid enters the domain, the temperature and thus sensible energy of PCM rises. Once the melting temperature is reached, the capsules begin to melt, and any further energy is stored into the PCM as latent heat. To ensure the complete melting of capsules, all the simulations were run for a sufficiently long duration. The material properties used for the simulations are specified in Table 1.

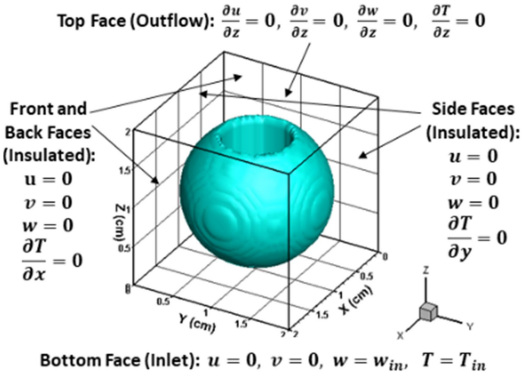

Figure 1: Domain and boundary conditions

Following are the assumptions made in the present analysis:

- Properties of paraffin and water are constant.
- Natural convection is implemented using Boussinesq approximation.
- The melting temperature is constant.
- The shell for PCM capsules is considered infinitely thin. Negligible thermal resistance is considered for the shell.
- The interface between the PCM and the HTF has been modelled by using a high artificial viscosity value of 10^{16} Ns⁄m^2 for the interface cells, thus suppressing the interfacial velocity to zero. This value of viscosity is arbitrarily chosen and any other high value which suppresses the velocity to zero at the interface can also be used.
- The channels pass precisely through the geometric center of individual capsules.

Table 1: Material properties

Parameter	Paraffin	Water
Density (ρ) (kg/m^3)	805	996
Dynamic viscosity (μ) (Ns/m^2)	3.65×10^{-3}	0.798×10^{-3}
Thermal conductivity (k) (W/mK)	0.22	0.615
Specific heat (C_p) (J/kgK)	2100	4178
Coefficient of thermal expansion (1/K)	3.08×10^{-4}	-
Melting point (T_m) (K)	333	-
Latent heat (L) (J/kg)	169×10^3	-

Internal channels are modeled within the PCM geometry by modifying the existing in-house codes used in previous research work by our group [9]. The encapsulation fraction parameter denoted using φ, is defined to account for the fraction of PCM material present inside each control volume. Mathematically speaking, $0 \leq \varphi \leq 1$. Table 2 indicates the modified values of outer radius of PCM capsule for increasing values of internal channel radius; all determined while maintaining constant total volume, equal to corresponding base capsule volumes without any internal channels.

For the present study, all the properties, such as density (ρ_{avg}), thermal conductivity (k_{avg}), and viscosity (μ_{avg}), are volume-averaged. Each of them can be expressed in terms of the encapsulation fraction (φ) as:

$$\rho_{avg} = \rho_{PCM}\,\varphi + \rho_{HTF}(1-\varphi) \quad (1)$$

$$k_{avg} = k_{PCM}\,\varphi + k_{HTF}(1-\varphi) \quad (2)$$

$$\mu_{avg} = \mu_{PCM}\,\varphi + \mu_{HTF}(1-\varphi) \quad (3)$$

The subscripts 'avg', 'PCM, and 'HTF', in the equations (1),(2), and (3) stand for average, PCM, and HTF, respectively.

Table 2: External radius of capsules for constant PCM volume

Base capsule radius(R_0) in mm	Modified outer radius of capsules (R_0) in mm			
	r/R_0 = 0.250	r/R_0 = 0.333	r/R_0 = 0.416	r/R_0 = 0.500
4.000	4.083	4.146	4.227	4.324
8.000	8.165	8.292	8.454	8.648

Considering the heat transfer model, a volume-averaged enthalpy-based energy conservation formulation, as indicated by equation (4) below, is used to describe the melting of the PCM

$$\frac{\partial}{\partial t}\left(\rho_{avg}H\right) + \nabla\cdot\left(\rho_{avg}\vec{v}H\right) = \nabla\cdot\left(K_{avg}\,\nabla\,T\right) \quad (4)$$

where,

$$H = \left[C_{P_{PCM}}\,\varphi + C_{P_{HTF}}(1-\varphi)\right]T + \varphi f L_f \quad (5)$$

In the above equation, f signifies the liquid fraction of PCM, which is the ratio of the amount of liquid PCM in a control volume to the total PCM present in the control volume, and L_f is the latent heat of melting. The energy equation (4) is discretized explicitly using the finite volume method, in which the values for velocity ($\vec{v}$) and temperature (T) are used from the previous time step for each new iteration. The discretization and numerical implementation scheme are similar to our previous work [10]. The discretized energy equation can be solved to obtain the new value of enthalpy (H_{new}). Upon substituting the value of H_{new} into equation (5) and choosing the value of temperature at the HTF-PCM interface as the melting temperature of PCM (T_m), the updated value of liquid fraction (f_{new}) is attained.

In continuation, f_{new} is utilized to obtain the temperature of the cell (T_{cell}). The value of T_{cell} varies with the value of the updated liquid fraction (f_{new}), for either of which, the following interpretations can be made:

- If the value of the liquid fraction obtained is less than zero, i.e., $f_{new} \le 0$ then $T_{cell} = \frac{H}{\left[C_{P_{PCM}}\,\varphi + C_{P_{HTF}}(1-\varphi)\right]}$. This indicates that the melting of PCM has not yet begun. The value of the liquid fraction assigned to the solver is 0.
- If liquid fraction obtained from (4) lies between 0 and 1, i.e., $0 < f_{new} < 1$ then the value of $T_{cell} = T_m$. This indicates that cells are at an interface of solid and liquid phases, and the value of the liquid fraction assigned to the solver is f_{new}.
- Finally, if the liquid fraction obtained from $f_{new} \ge 1$, $T_{cell} = \frac{H - \varphi L_f}{\left[C_{P_{PCM}}\,\varphi + C_{P_{HTF}}(1-\varphi)\right]}$. This further indicates that the cells have completely melted, and the value of the liquid fraction assigned to the solver is 1.

Similarly, considering the fluid flow model, the fluid flow is considered in the heat transfer fluid and the liquid PCM. As shown in equations (6) and (7) below, the continuity and momentum conservation equations are modified to incorporate the effect of different phases. The equations are solved by using the SIMPLER algorithm.

$$\nabla\cdot\vec{v} = 0 \quad (6)$$

$$\rho_{avg}\frac{\partial\vec{v}}{\partial t} + \rho_{avg}(\vec{v}\cdot\nabla)\vec{v} = -\nabla P + \mu_{avg}\nabla^2\vec{v} + \vec{S_B} + \tau\vec{v} \quad (7)$$

In equation (7), P refers to the pressure at the center of each control volume. The source term due to Boussinesq approximation is given by: $\vec{S_B} = \rho_{PCM}\vec{g}\alpha\varphi(T_{cell} - T_m)$. $\vec{g}$ and α denote acceleration due to gravity, and the thermal expansion coefficient, respectively. $\vec{S_B}$ is non-zero only if $T_{cell} > T_m$. The term $\tau\vec{v}$ forces the velocity to become zero in the solid PCM region [10].

4. RESULTS AND DISCUSSION

The entire formulation is implemented by modifying the in-house code used previously for the study presented in Athawale et al. [11]. The validation of the code was carried out by Athawale et al. [11] with the existing work of Khodadadi and Zhang [1].

Liquid fraction contours for PCM with 4 mm and 8 mm radii at 50 s are shown in Figures 2 and 3, respectively. It is observed that, upon increasing the channel size, while maintaining constant volume, a quicker melting is observed due to higher effective heat transfer surface area.

Corresponding temperature contours at 50 s are shown in Figures 4 and 5, respectively. It can be seen that it is a case of non-uniform heat transfer since the melting starts from the bottom, where the HTF comes into contact with the capsules first. The HTF then proceeds through the periphery and the internal channels and melts the PCM completely. For the lower radius channels the temperature in the PCM is lower indicating less heat transfer to the internal parts of the capsule. This is more prominent for the 8 mm cases. Faster melting at the bottom and thermal stratification forming at the top resulting in increased heat storage efficiency, similar to [12] was also observed.

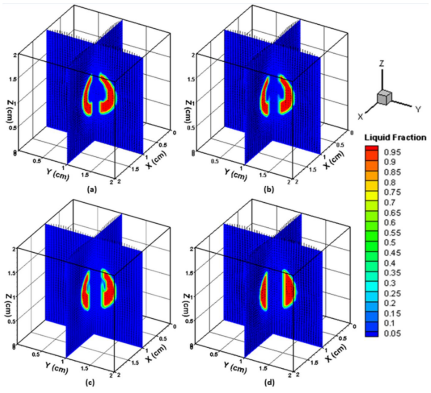

Figure 2: Liquid fraction contours for PCM with 4 mm base radius (a) $r/R_0 = 0.250$, (b) $r/R_0 = 0.333$, (c) $r/R_0 = 0.416$, (d) $r/R_0 = 0.500$ at 50 s

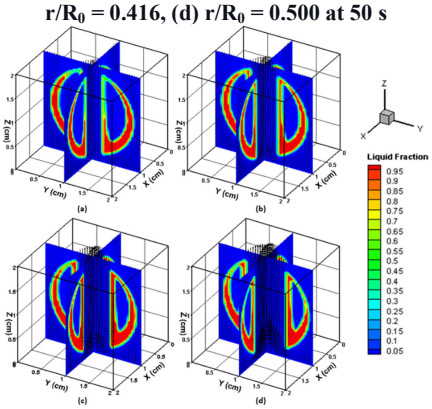

Figure 3: Liquid fraction contours for PCM with 8 mm base radius (a) $r/R_0 = 0.250$, (b) $r/R_0 = 0.333$, (c) $r/R_0 = 0.416$, (d) $r/R_0 = 0.500$ at 50 s

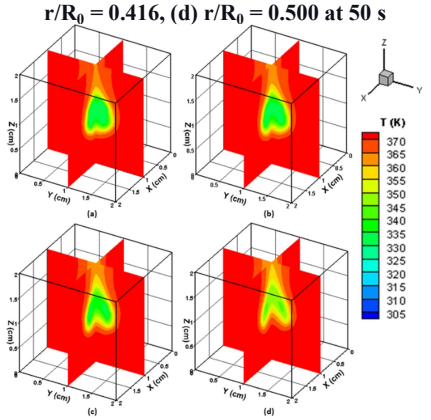

Figure 4: Temperature contours with 4 mm base radius (a) $r/R_0 = 0.250$, (b) $r/R_0 = 0.333$, (c) $r/R_0 = 0.416$, (d) $r/R_0 = 0.500$ at 50 s

Figure 6 represents the variation of liquid fraction with time for all the cases. For the capsules with 4 mm base radius and r/R_0 as 0.250, 0.333, 0.416, and 0.500, a decrement in melting duration by 13.02%, 19.75%, 30.05%, and 42.58% with respect to the base case is observed. Similarly, for the capsules with 8 mm base radius and r/R_0 as 0.250, 0.333, 0.416, and 0.500, a decrement in melting duration by 33.64%, 42.08%, 47.93%, and 51.15% with respect to the base case is observed. These values indicate that the melting duration reduces much more rapidly in capsules having larger internal flow channels and larger external radii.

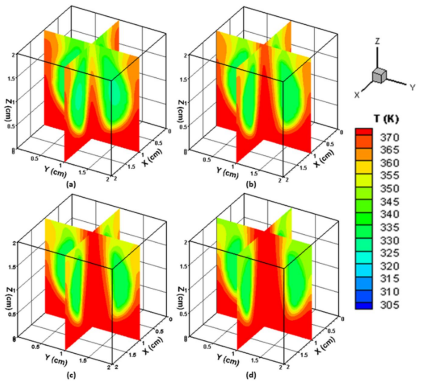

Figure 5: Temperature contours with 8 mm base radius (a) $r/R_0 = 0.250$, (b) $r/R_0 = 0.333$, (c) $r/R_0 = 0.416$, (d) $r/R_0 = 0.500$ at 50 s

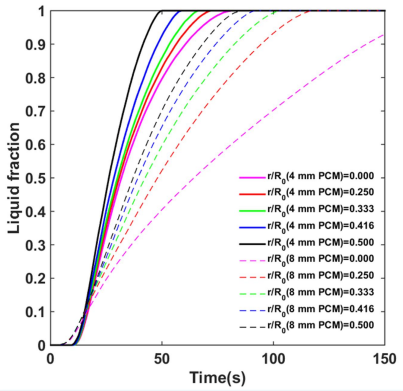

Figure 6: Variation of liquid fraction with time

Figures 7 and 8 indicate the variation of latent, sensible, and total energies for the capsules with 4 mm and 8 mm base radii, respectively. The latent energy for all the 4 mm cases settles at 36.47 J. The sensible energy increases with an increase in channel radius, because of the PCM's higher effective heat transfer area, arising due to an increasing nature of internal channel size. The latent energy for all the 8 mm cases settles at 291.76 J. The sensible energy trend for the 8 mm cases can be understood using similar arguments proposed for Fig. 7(b).

Figure 9 represents the latent energy fraction (latent energy / total energy) plotted against time for all the cases combined. From the plot, the latent energy fraction of cases corresponding to 4 mm capsules begins to rise after a lag compared to the 8 mm capsules. Since the capsules are located at the center of the cubical domain, the HTF comes into

contact with the capsules for the 8 mm cases earlier than the 4 mm cases. The 4 mm cases peak earlier and the peak values are higher than the 8 mm cases, owing to their lesser volume, resulting in quicker complete melting. Finally, the latent energy fraction for the 8 mm PCM cases is higher indicating lesser sensible energy storage due to longer melting period. Additionally, the base cases have lower sensible energy content due to less effective heat transfer when compared to PCMs having internal channels. Thus their latent energy fraction is higher upon complete melting although the trends for the peak values are reversed.

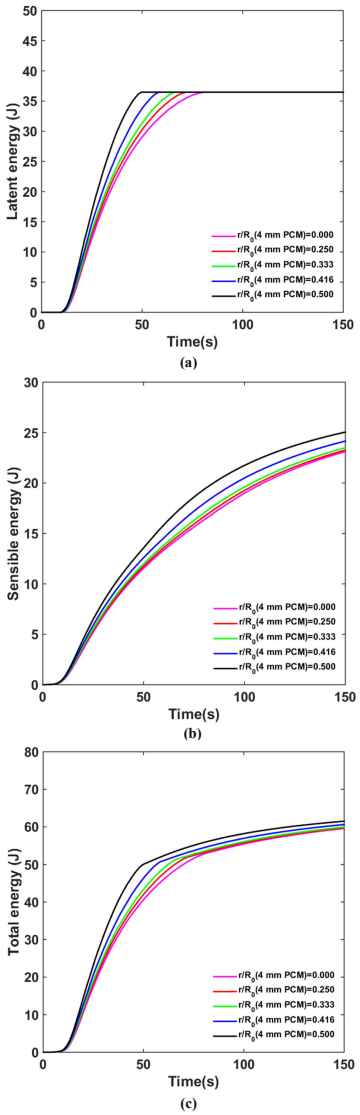

Figure 7: Variation of (a) latent energy, (b) sensible energy, (c) total energy of PCM with time for 4 mm base radius

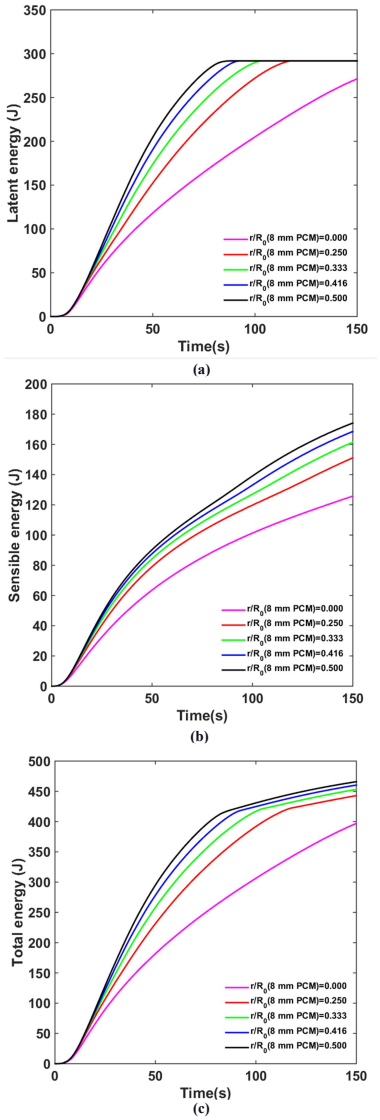

Figure 8: Variation of (a) latent energy, (b) sensible energy, (c) total energy of PCM with time for 8 mm base radius

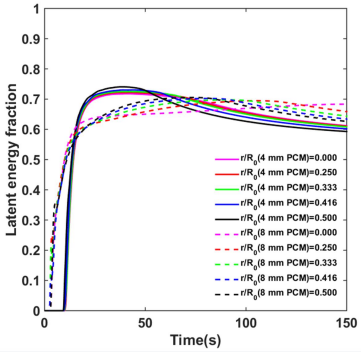

Figure 9: Variation of latent energy fraction with time

5. CONCLUSIONS

The energy storage characteristics, in terms of liquid fraction, latent, sensible, and total energies for spherical encapsulated PCMs with internal cylindrical channels and constant total volume, have been analyzed in this paper. The melting duration reduces by 13.02%, 19.75%, 30.05%, and 42.58% with respect to the capsule having a base radius of 4 mm. Similarly, melting duration reduces by 33.64%, 42.08%, 47.93%, and 51.15% with respect to the capsule having a base radius of 8 mm. These values show that the melting duration reduces faster with increase in channel radius ratio for larger capsules. Thus, having internal channels for macro-encapsulated PCM systems with larger capsules is more effective. The work can be extended to a packed bed system containing multiple capsules arranged in a structured manner for further analysis.

NOMENCLATURE

avg	Volume average	
C_p	Specific heat	
f	Liquid fraction	
H	Specific enthalpy	[J/kg]
K	Thermal conductivity	[W/mK]
L	Latent energy	[J/kg]
P	Pressure	[N/m]
T	Temperature	[K]
T_m	Melting temperature	[K]
v	Velocity	[m/s]
α	Coefficient of thermal expansion	[1/K]
ρ	Density	[kg/m^3]
μ	Viscosity	[Ns/m^2]

ACKNOWLEDGEMENTS

This work has been supported by DST (Department of Science and Technology) SERB project CRG/2021/003780.

REFERENCES

[1] J. M. Khodadadi, and Y. Zhang, Effects of buoyancy-driven convection on melting within spherical containers, International Journal of Heat and Mass Transfer, 44(8), 2001, pp. 1605-1608.

[2] A.F. Regin, S.C. Solanki, and J.S. Saini, Latent heat thermal energy storage using cylindrical capsule: Numerical and experimental investigations, Renewable Energy, 31(13), 2006, pp.2025-2041.

[3] S. Kalaiselvam, M. Veerappan, A.A Aaron, and S. Iniyan, Experimental and analytical investigation of solidification and melting characteristics of PCMs inside cylindrical encapsulation. International Journal of Thermal Sciences, 47(7), 2008, pp. 858-874.

[4] F. Agyenim, N. Hewitt, P. Eames, and M. Smyth, A review of materials, heat transfer and phase change problem formulation for latent heat thermal energy storage systems (LHTESS), Renewable and Sustainable Energy Reviews, 14(2), 2010, pp. 615-628.

[5] M. Hlimi, S. Hamdaoui, M. Mahdaoui, T. Kousksou, A.A Msaad, A. Jamil, and A. El Bouardi, Melting inside a horizontal cylindrical capsule, Case Studies in Thermal Engineering, 8, 2016, pp. 359-369.

[6] Z. Liu, Z. J. Yu, T. Yang, D. Qin, S. Li, G. Zhang, F. Haghighat, and M.M. Joybari, A review on macro-encapsulated phase change material for building envelope applications, Building and Environment, 144, 2018, pp. 281-294.

[7] J. Bony, and S. Citherlet, Numerical model and experimental validation of heat storage with phase change materials. Energy and Buildings, 39(10), 2007, pp. 1065-1072.

[8] H. Sattari, A. Mohebbi, M. M Afsahi, and A. A. Yancheshme, CFD simulation of melting process of phase change materials (PCMs) in a spherical capsule. International Journal of Refrigeration, 73,2017, pp. 209-218.

[9] B. V. S. Dinesh, and A. Bhattacharya, Effect of foam geometry on heat absorption characteristics of PCM-metal foam composite thermal energy storage systems, International Journal of Heat and Mass Transfer, 134, 2019, pp. 866-883.

[10] V. Athawale, A. Bhattacharya, and P. Rath, Prediction of melting characteristics of encapsulated phase change material energy storage systems, International Journal of Heat and Mass Transfer, 181, 2021, pp. 121872.

[11] V. Athawale, A. Jakhar, M. Jegatheesan, P. Rath, and A. Bhattacharya, A 3D resolved-geometry model for unstructured and structured packed bed encapsulated phase change material system. Journal of Energy Storage, 51, 2022, pp. 104430.

[12] V. Soni, A. Kumar, and V. K. Jain, Modeling of PCM melting: Analysis of discrepancy between numerical and experimental results and energy storage performance. Energy 150, 2018, pp. 190-204.